European Cells and Materials Vol.47 2024 (pages 109–124) DOI: 10.22203/eCM.v047a08 ISSN 1473-2262

Original Article

EXTRACELLULAR MATRIX FROM HIPSC-MESENCHYMAL PROGENITORS MODULATES THE THREE-LINEAGE DIFFERENTIATION OF HUMAN BONE MARROW STROMAL CELLS

D. Hanetseder[1,2], B. Schaedl[1,2,3], H. Redl[1,2] and D. Marolt Presen[1,2,*]

[1]Ludwig Boltzmann Institute for Traumatology, The Research Centre in Cooperation with AUVA, A-1200 Vienna, Austria
[2]Austrian Cluster for Tissue Regeneration, A-1200 Vienna, Austria
[3]University Clinic of Dentistry, Medical University of Vienna, A-1090 Vienna, Austria

Abstract

Mesenchymal stromal cells from the bone marrow (BMSCs) exhibit a functional decline during aging. We previously found that extracellular matrix (ECM) engineered from human induced pluripotent stem cell-derived mesenchymal progenitors enhances the osteogenic capacity of BMSCs. In the current study, we investigated how this ECM affects the three-lineage differentiation and secretory activity of BMSCs. BMSCs were seeded on the ECM layer and osteogenic, adipogenic and chondrogenic lineages were induced in monolayer or micromass cultures. Differentiation responses were compared to controls on tissue culture plastic after 21 days, and secretion of interleukin 6 was evaluated after 3 and 21 days of culture. We found a significant increase in BMSC growth on the ECM in all three differentiation media compared with controls. Osteogenic cultures on the ECM resulted in significantly higher alkaline phosphatase activity, osteogenic gene expression, collagen deposition, and matrix mineralization. In adipogenic cultures, a significant decline in adipocyte formation was found on the ECM. Chondrogenic induction on the ECM resulted in significantly increased chondrogenic gene expression, glycosaminoglycans deposition and collagen type II deposition, and no significant increase in collagen type X gene expression compared to control. Secretion of interleukin 6 was modulated by the three differentiation media and culture surface, and was reduced after 21 days of osteogenic and chondrogenic induction on the ECM. Together, our data suggest that engineered ECM modulates BMSCs trilineage differentiation toward enhanced osteogenesis and chondrogenesis, and reduced adipogenesis. Thus, our ECM might provide a bioactive component for enhancing osteochondral regeneration in older patients.

Keywords: Extracellular matrix, iPSCs, bone marrow stromal cells, osteogenic, chondrogenic, adipogenic differentiation.

***Address for correspondence**: D. Marolt Presen, Ludwig Boltzmann Institute for Traumatology, The Research Centre in Cooperation with AUVA, A-1200 Vienna, Austria; Austrian Cluster for Tissue Regeneration, A-1200 Vienna, Austria. Email: darjamarolt@gmail.com

Introduction

Mesenchymal stromal cells (MSCs) are extensively studied for their therapeutic potential in tissue regeneration (Dominici *et al*., 2006; Krampera and Le Blanc, 2021). Among various adult and perinatal tissue sources of MSCs, bone marrow is one of the most commonly used and best characterized sources for bone regeneration (Marolt Presen *et al*., 2019). Bone marrow-derived MSCs (BMSCs) were shown to self-renew, give rise to bone, bone marrow stroma, cartilage, adipose tissue and other mesodermal lineages, and to aid in tissue regeneration via their secretory activity (Bianco *et al*., 2006; Kuznetsov *et al*., 2019; Murphy *et al*., 2013; Pittenger *et al*., 1999; Sacchetti *et al*., 2007).

Therapeutic use of MSCs requires a sufficient number of cells with adequate regenerative potential. It is known that MSC origin (Frobel *et al*., 2014; Kern *et al*., 2006; Lapasset *et al*., 2011; Mensing *et al*., 2011; Vidal *et al*., 2006, 2007), chronological age of the donor and extended *in vitro* cultivation can affect the number and functional properties of MSCs (Bruder *et al*., 1997; Fernandez-Rebollo *et al*., 2020; Stolzing *et al*., 2008; Wagner *et al*., 2009; Zupan *et al*., 2021). Various "biomimetic" strategies have been investigated to enhance MSC functionality, including *in vitro* culture on protein substrates and in three-dimensional (3D) biomaterial scaffolds as well as application of biochemical and biophysical signals with recognized roles in cell differentiation and tissue development (Freytes *et al*., 2009).

In native tissues, MSCs are surrounded by an abundant extracellular matrix (ECM), a complex network of proteins, proteoglycans and glycosaminoglycans (Arnott *et al*., 2011; Assunção *et al*., 2020; Coleman *et al*., 2013; Prewitz *et al*., 2013; Unsicker *et al*., 2013). The ECM provides structural support to the cells and acts as a reservoir and regulator of growth factor activity in a tissue-specific manner (Gresham *et al*., 2020; McKee *et al*., 2019; Yong *et al*., 2020). ECM regulates cell migration, proliferation, differentiation and autophagy, and influences stem cell fate and immunological responses (Fitzpatrick and McDevitt, 2015; Hynes and Naba, 2012; Rozario and DeSimone, 2010).

In order to mimic this complex microenvironment *in vitro* and enhance the number and functionality of MSCs, ECM has been engineered in various formats, including thin layers on cell culture dishes, coatings of 3D scaffolds and scaffolds composed entirely of cell-derived ECM (Ang *et al*., 2014; Lai *et al*., 2010; Lin *et al*., 2012; Lu *et al*., 2011; Tang *et al*., 2014; Zhang *et al*., 2016). ECM layers generated from human and mouse BMSCs were shown to enhance MSC proliferation and maintain their colony forming- and differentiation potentials (Lai *et al*., 2010; Lin *et al*., 2012; Sun *et al*., 2011). ECM layers generated from human fetal bone marrow MSCs, human adult bone marrow MSCs and human neonatal dermal fibroblasts enhanced MSC osteogenic and chondrogenic differentiation compared with standard tissue culture plastic (Lin *et al*., 2012; Ng *et al*., 2014; Pei *et al*., 2011), as well as maintained the chondrogenic phenotype of cultured chondrocytes (Yang *et al*., 2018). Rabbit BMSC-derived ECM scaffolds enhanced the thickness and homogeneity of cartilaginous tissue engineered *in vitro* from autologous rabbit chondrocytes (Tang *et al*., 2013). It was also shown that ECM supports adipogenic differentiation of MSCs (Ang *et al*., 2014; Mariman and Wang, 2010; Narayanan *et al*., 2018). In particular, ECM generated from BMSCs in adipogenic medium under macromolecular crowding conditions strongly enhanced subsequent BMSC differentiation into the adipogenic lineage compared with a standard differentiation model on tissue culture plastic (Ang *et al*., 2014).

Unlike primary cell sources used in previous studies, human induced pluripotent stem cells (hiPSCs) represent an unlimited source of youthful human MSC-like progenitors (hiPSC-MPs) for ECM engineering (Frobel *et al*., 2014; Lapasset *et al*., 2011; Lian *et al*., 2010; de Peppo *et al*., 2013; Sheyn *et al*., 2016). hiPSC-based production of progenitor cells and tissue components can be standardized and scaled up for research studies and eventual clinical translation (Frobel *et al*., 2014; Lian *et al*., 2010; de Peppo *et al*., 2013). In our previous study, we found that ECM engineered from hiPSC-MPs enhanced osteogenic differentiation of young adult and aged BMSCs compared to tissue culture plastic and single protein substrate coatings (Hanetseder *et al*., 2023). In the current study, we aimed to evaluate whether cultivation of BMSCs on hiPSC-MP-derived ECM influences not only osteogenic but also adipogenic and chondrogenic differentiation. We hypothesized that culturing on hiPSC-MP-ECM will shift the balance of trilineage differentiation and affect the secretory activity of differentiating BMSCs in comparison to BMSCs cultured on tissue culture plastic.

Materials and Methods

Materials

All materials and reagents were purchased from Sigma Aldrich (St. Louis, MO, USA) unless otherwise stated.

Cell Culture

hiPSC-MPs were generated and characterized in detail for the expression of MSC-related surface antigens and differentiation potential in our previous study (de Peppo *et al*., 2013). The cells were seeded on standard tissue culture flasks pre-coated with 0.1 % gelatin solution and expanded in KnockOut Dulbecco's modified Eagle's medium (KO-DMEM), supplemented with 20 % HyClone fetal bovine serum (FBS), 2 mM GlutaMAX, 0.1 mM nonessential amino acids, 0.1 mM β-mercaptoethanol (all from Fisher Scientific, Pittsburgh, PA, USA), 100 U/mL penicillin-streptomycin (P/S) and 1 ng/mL basic fibroblast growth factor (b-FGF) (Invitrogen, Fisher Scientific). The cells were cultured in a humidified incubator at 37 °C and 5 % CO_2 with media changes twice per week until confluent.

Bone marrow mononuclear cells of a 20-year-old female donor were purchased from Lonza (Basel, Switzerland) and seeded on tissue culture plates. Cells from the same young adult donor were used in our prior study (Hanetseder *et al*., 2023). Non-adherent cells were removed with media changes and adherent cells, i.e., BMSCs, were expanded in medium consisting of Dulbecco's modified Eagle's medium high glucose (DMEM-HG), supplemented with 10 % FBS, 100 U/mL P/S, 2 mM L-glutamine and 1 ng/mL b-FGF (PeproTech®, Fisher Scientific) with regular media changes twice per week. Upon confluence, BMSCs were passaged and characterized to confirm the expression of MSC surface antigens and the trilineage differentiation potential according to the consensus position statement by the International Society for Cellular Therapy (Dominici *et al*., 2006) (data not shown). Cells of passage 5 were used in the following experiments.

Generation of hiPSC-MP-ECM Layer

hiPSC-MP-ECM layer was generated and decellularized as described in our previous study (Hanetseder *et al*., 2023). Briefly, cells were seeded on 24-well plates at 19.000 cells/well and cultured in ECM medium consisting of DMEM-HG, 10 % FBS, 100 U/mL P/S, 2 mM L-glutamine and 50 µM ascorbic acid-2-phosphate (A2P) for ten days, when the formation of a dense ECM layer was confirmed. ECM was washed with phosphate-buffered saline (PBS) without Ca^{2+} and Mg^{2+} (Lonza) and decellu-

larized by incubation in 0.5 % Triton X-100 buffer containing 20 mM NH_4OH in PBS for 15 min at 37 °C. After washing with PBS, ECM was incubated in 100 U/mL DNase I solution in DPBS for 1 h. Decellularized ECM was washed and stored until use in PBS containing 100 U/mL P/S at 4 °C.

Trilineage Differentiation of BMSCs on the ECM Layer

All differentiation experiments were conducted using the same control medium consisting of DMEM-HG with 10 % FBS, 2 mM L-glutamine and 100 U/mL P/S) or a specific differentiation medium.

To induce osteogenic differentiation, BMSCs were seeded at a density of 5000 cells/cm^2 on tissue culture plastic or ECM layer in 24-well plates, and cultured for up to 42 days in either control medium or osteogenic differentiation medium consisting of control medium further supplemented with 10 nM dexamethasone, 50 µM ascorbic acid 2-phosphate (A2P) and 10 mM ß-glycerophosphate.

To induce adipogenic differentiation, BMSCs were seeded at a density of 7400 cells/cm^2 on tissue culture plastic or ECM layer in 24-well plates, and cultured for up to 21 days in adipogenic differentiation medium consisting of control medium further supplemented with 0.5 mM 3-Isobutyl-1-methylxanthine (Serva, Heidelberg, Germany), 60 µM indomethacin, 0.5 µM hydrocortisone and 1 µM dexamethasone. Higher cell density in the adipogenic group was used as an additional stimulus for adipogenic differentiation. For the adipogenic differentiation control groups, the cells were seeded at a density of 5000 cells/cm^2 on both surfaces and cultured in control medium.

To induce chondrogenic differentiation, BMSCs were seeded as cell micromasses consisting of 100.000 cells/20 µL droplet of control medium on tissue culture plastic or ECM layer in 24-well plates. The micromasses were allowed to adhere for 1 h before adding culture medium. The micromasses were cultured for up to 21 days in either control medium or in chondrogenic differentiation medium consisting of DMEM-HG supplemented with 40 µg/mL L-proline, 100 nM dexamethasone, 50 µg/mL A2P, 1 % insulin-transferrin-selenium-ethanolamine (ITS-X mix 100x), 0.91 mM sodium pyruvate and 1 % P/S (all from Thermo Fisher) and 10 ng/mL human transforming growth factor-β3 (TGF-β3) HumanKine®.

DNA Content Quantification

For DNA content quantification, the BMSC cultures were washed with PBS and incubated in a digestion buffer containing 150 mM NaCl, 55 mM Na Citrate, 20 mM EDTA, 0.2 M NaH_2PO_4 (Honeywell Research Chemicals, Morris Plains, NJ, USA), 10 mM EDTA, 6 U/mL papain, and 10 mM cysteine in ddH_2O (with pH 6.0) overnight at 60 °C. The digested samples were collected, centrifuged for 5 min at 300 ×g, and DNA content of the supernatant was determined using Hoechst 33342 dye. 100 µL of Hoechst working solution consisting of 5 µg/mL Hoechst dye in assay buffer (2 M NaCl, 50 mM NaH_2PO_4, pH 7.4) were added to 50 µL of samples or calf thymus DNA standards of known concentration. Samples were incubated for 5 min at 37 °C in the dark while slowly shaking, and fluorescence was measured at 355/460 nm using POLARstar Omega microplate reader (BMG LABTECH, Ortenberg, Germany). DNA concentration of the samples was determined using a standard curve constructed with DNA solutions of known concentrations.

Alkaline Phosphatase Activity Assay

To determine alkaline phosphatase (ALP) activity, the culture medium was aspirated, then the cells were washed with PBS and stored at – 80 °C prior analysis. The cells were thawed and extracted by adding the cell lysis solution containing 0.5 % Triton X-100 in 0.5 M 2-amino-2-methyl-1-propanol buffer with 2 mM $MgCl_2$ with a pH 10.3. The lysed cells were centrifuged for 5 min at 300 ×g, and the ALP activity of the supernatant was determined by incubation with 0.02 M para-Nitrophenylphosphate (pNPP) substrate solution at 37 °C. The reaction time until development of yellow color was noted and the reaction was stopped by adding 0.2 M NaOH stop solution. The sample absorbance at 405 nm was measured with the POLARstar Omega microplate reader. ALP activity was determined using a standard curve constructed with p-nitrophenol solutions of known concentrations.

Glycosaminoglycans Content Quantification

For glycosaminoglycans (GAG) content quantification, culture medium was aspirated from BMSC cultures, samples were washed with PBS and stored at – 20 °C prior to analysis. Upon thawing, samples were digested as described for the DNA content determination in Trilineage differentiation of BMSCs on the ECM layer. Afterwards, digested samples were collected, centrifuged for 5 min at 300 ×g, and GAG content of the supernatant was determined using Blyscan sulfated glycosaminoglycan assay (BioColor, B1000, Mid and East Antrim, UK) following the manufacturer's instructions. Optical density of the samples was determined at 656 nm using the POLARstar Omega microplate reader, and GAG concentration of the samples was determined using a standard curve constructed with GAG solutions of known concentrations.

Gene Expression Analyses

RNA extraction was performed using the QIAGEN RNeasy Mini Kit (QIAGEN, Hilden, Germany), followed by DNase treatment (Thermo Fisher Scientific, Waltham, MA, USA) according to the manufacturer's instructions. Approx. 200 ng of extracted RNA was transcribed into cDNA with the GoScript™ Reverse Transcription System 100 (Promega, Madison, WI, USA) using random hexamer primers. Real-time PCR was

performed using the CFX96 Real-Time PCR Detection System (Bio-Rad Laboratories, Hercules, CA, USA). 2 µL of cDNA were added to a 25 µL volume reaction containing the TaqMan® universal PCR master mix and one of the TaqMan® Gene Expression Assays (Thermo Fisher Scientific) for alkaline phosphatase (ALP; Hs01029144_m1), osteopontin (SPP1; Hs00959010_m1), bone sialoprotein (IBSP; Hs00173720_m1), osteocalcin (Hs01587814_g1), peroxisome proliferator activated receptor gamma (PPARG, Hs01115513_m1), adiponectin (ADIPOQ, Hs00605917_m1), fatty acid binding protein 4 (FABP4, Hs01086177_m1), lipoprotein lipase (LPL, Hs00173425_m1), Collagen type II (COL2A1, Hs00264051_m1), Aggrecan (ACAN, Hs00153936_m1), Collagen type X (COL10A1, Hs00166657_m1), SRY-box 9 (Sox9, Hs00165814_m1), runt related transcription factor 2 (RUNX2, Hs04940094_m1), Sp7 transcription factor (OSX, Hs00541729_m1) and glyceraldehyde 3-phosphate dehydrogenase (GAPDH, Hs02786624_g1). Standard cycling conditions were applied: 95 °C for 10 min, followed by 40 cycles of 95 °C for 15 s (denaturation) and 60 °C for 60 s (annealing and extension). Results were exported using the CFX Manager 3.1 (Bio-Rad Laboratories) and analyzed in Excel (Microsoft, Redmond, WA, USA) according to the ΔΔCt method. Expression levels of the target genes were normalized to the expression level of the housekeeping gene GAPDH.

Histological Analyses of Monolayer Cultures

Upon differentiation, the BMSC culture samples were washed with PBS and fixed with 4 % formaldehyde in PBS for 10 min at RT. Following staining procedures described below, results were documented using inverted microscope fitted with color camera (Zeiss Primovert Microscope with ICc5 AxioCam).

Alizarin Red staining was used to visualize calcium deposition 42 days after the osteogenic differentiation of BMSCs. The samples were washed with distilled water and incubated in 2 % Alizarin Red S solution (pH 4.2) for 30 min. Afterwards, Alizarin Red S solution was removed, the samples were extensively rinsed with distilled water, and analyzed.

Adipogenic differentiation of BMSCs was visualized using Oil Red O staining. 3 g/L Oil Red O stock solution was prepared by dissolving in 2-propanol. The samples were washed with distilled water, followed by a wash with 70 % EtOH, and incubation in Oil Red O working solution (stock solution 3:2 in ddH_2O) for 15 min at RT. Then, Oil Red O working solution was removed and samples were washed with distilled water. For quantification, eight non-overlapping images were taken for each of the four groups and the number of adipocytes was determined.

Histological/Immunohistochemical Analyses of Micromass Cultures

Upon chondrogenic differentiation, BMSC micromasses were washed with PBS and fixed in 4 % phosphate buffered formaldehyde (Roti®-Histofix 4 %, P087.3, Carl Roth, Karlsruhe, Germany) for 24 h. The samples were then rinsed, dehydrated in an increasing series of EtOH concentrations and embedded in paraffin using a Vacuum Infiltration Processor (Tissue Tek, Sakura Finetek, Nagano, Japan). 4 µm thin sections were prepared using a microtome (Thermo Scientific Microm HM 355 S, Thermo Fisher Scientific, Waltham, MA, USA), placed on glass slides and kept at 37 °C overnight for optimal attachment of the sections to the glass slides.

To determine the presence of glycosaminoglycans, Alcian blue staining was performed. The samples were incubated in the Alcian blue staining solution (0.1 % in 3 % acetic acid at pH 2.5) for 30 min, rinsed with distilled water and the nuclei were counter-stained with Haemalaun (Haemalaun after Mayer, T865.3, Carl Roth, Karlsruhe, Germany).

To determine the presence of collagen type II, immunohistochemical staining was performed. The sections were rehydrated in a descending EtOH series and Aqua dest. Antigen retrieval was conducted using pepsin treatment (Pepsin Reagent Antigen Retriever, R2283, Merck KGaA, Darmstadt, Germany) for 10 min at 37 °C in a humidified chamber. The sections were then incubated with primary antibody against collagen type II (MS 306-P1; Collagen II Ab-3 (Clone 6B3) mouse monoclonal antibody, Thermo Fisher Scientific, Waltham, MA, USA) for one hour at RT. Upon washing, the samples were incubated with HRP-anti-mouse secondary antibody (Bright Vision poly HRP-Anti-Mouse IgG, VWRKDPVM110HRP, ImmunoLogic, Duiven, Netherlands) for 30 min at RT. Signal was detected using NovaRed® HRP peroxidase substrate kit (ImmPACTTMNova RedTM, SK4805, Vector Laboratories, Burlingame, CA, USA) according to the manufacturer's instructions, and the nuclei were stained with Haemalaun.

The stained samples were imaged using light microscopy (Axioplan2 imaging, Carl Zeiss Microscopy, Oberkochen, Germany and Olympus BX61VS, Olympus Corporation, Tokyo, Japan).

Determination of Interleukin 6 Content

Supernatants were harvested from osteogenic, adipogenic and chondrogenic BMSC cultures and their respective counterparts in control medium on the ECM and tissue culture plastic at day 3 and day 21, both times 2 days post medium change. The concentrations of interleukin 6 (IL-6) were determined by using Quantikine® ELISA kit (R&D Systems, Minneapolis, MN, USA) according to the manufacturer's instructions, using a standard curve constructed with standards of known concentrations contained in the kit.

Statistical Analyses

All data are presented as averages ± standard deviation (SD). Normal data distribution was evaluated, and differences between groups were evaluated accordingly using either one-way Kruskal–Wallis test with Dunn's multiple comparison test, one-way ANOVA or two-way ANOVA with Tukey's multiple comparison test, with a *p*-value of 0.05 considered as statistically significant. The number of samples evaluated in different experiments was 4–8, as noted in the figure legends. All analyses were performed using GraphPad Prism 9 software (GraphPad Software, San Diego, CA, USA)

Results

hiPSC-MP-ECM Enhances Human BMSC Proliferation in Different Culture Conditions

Human BMSCs were grown on ECM layer and on tissue culture plastic in control, osteogenic, adipogenic and chondrogenic differentiation media for up to 21 days (Fig. 1). After 5 days of culture, enhanced cell growth on the ECM layer could be observed in control, osteogenic and adipogenic media compared to cells growing on tissue culture plastic (Fig. 1**A,B**). At the same timepoint, BMSCs growing in micromass cultures in control medium on the ECM layer exhibited a flat and more aligned morphology compared to micromass cultures growing in control medium on tissue culture plastic. Micromass cultures in chondrogenic medium on the ECM layer remained attached and exhibited a round cell morphology, whereas micromass cultures in chondrogenic medium on tissue culture plastic started to detach from the surface and formed pellets (Fig. 1**C**). DNA content quantification indicated a significantly higher BMSC proliferation in control, osteogenic and adipogenic media on the ECM layer compared to tissue culture plastic after 14 and 21 days (Fig. 1**D,E**). For BMSC micromass cultures in control medium, no significant difference in DNA content could be observed between cultures on the ECM layer and tissue culture plastic (Fig. 1**F**). However, DNA content of BMSC micromass cultures in chondrogenic medium on the ECM layer was significantly higher compared to tissue culture plastic after 14 and 21 days (Fig. 1**F**). Taken together, our data suggest that culture on hiPSC-MP-ECM layer enhances proliferation of human BMSCs growing both in control medium in monolayer culture, as well as in differentiation media in monolayer or micromass cultures.

hiPSC-MP-ECM Enhances Osteogenic Differentiation of Human BMSCs

We next evaluated osteogenic differentiation markers of human BMSCs growing on ECM layer and on tissue culture plastic in control and osteogenic differentiation media for up to 42 days (Fig. 2). Gene expression analysis showed a significant upregulation of *ALP*, *SSP1*, *BSP* and *OCN*, as well as transcription factors *OSX* and *RUNX2*, after 21 days of culture in osteogenic differentiation medium on the ECM as compared to tissue culture plastic (Fig. 2**A**). There were no significant differences in *OSX* expression between the ECM and plastic groups in other differentiation conditions, whereas *RUNX2* was significantly downregulated in adipogenic cultures on ECM as compared to tissue culture plastic (**Supplementary Fig. 1**). Analysis of ALP enzyme activity after 14 and 21 days of culture showed a significant upregulation in osteogenic differentiation medium on the ECM as compared to tissue culture plastic (Fig. 2**B**), whereas ALP activity normalized to DNA content was not significantly different between the two groups (**Supplementary Fig. 2**). Furthermore, Alizarin red staining showed a markedly higher calcium deposition by human BMSCs cultured in osteogenic differentiation medium for 42 days on the ECM as compared to the tissue culture plastic (Fig. 2**C**). Taken together, these data show a strong enhancement of early and late osteogenic markers in BMSCs differentiating on the ECM layer.

hiPSC-MP-ECM Reduces Adipocyte Formation by Human BMSCs

We next determined adipogenic differentiation markers of human BMSCs growing on ECM layer and on tissue culture plastic in control and adipogenic differentiation media for up to 21 days (Fig. 3). Expression of all four adipogenic marker genes was markedly higher in BMSCs growing in adipogenic differentiation medium compared to control medium on both ECM layer and tissue culture plastic after 21 days of culture. In adipogenic differentiation medium, gene expression levels of *PPARG* and *ADIPOQ* genes were comparable between BMSCs cultured on the ECM layer and tissue culture plastic, whereas *FABP 4* and *LPL* genes indicated a trend of lower gene expression on the ECM layer compared to tissue culture plastic (Fig. 3**A**).

Interestingly, quantification of cells stained positively by Oil Red O showed a significant decrease in the formation of lipid-containing adipocytes after 10, 15 and 21 days of culture in adipogenic medium on the ECM layer compared to tissue culture plastic (Fig. 3**B,C**). No lipid-containing adipocytes were found in control medium on both culture surfaces. Taken together, these data suggest a decrease in adipogenic differentiation of BMSCs on the ECM layer.

hiPSC-MP-ECM Enhances Chondrogenic Differentiation of Human BMSCs

We next determined chondrogenic differentiation markers of human BMSCs growing on ECM layer and on tissue culture plastic in micromass cultures in control and chondrogenic differentiation media for up to 21 days (Fig. 4). Gene expression analysis showed a significant upregulation of *Col II*, *Sox 9* and *ACAN* gene expression after 21 days in chondrogenic culture conditions on the ECM as compared to tissue culture plastic (Fig. 4**A**). In contrast, gene expression of *Col X* showed no significant dif-

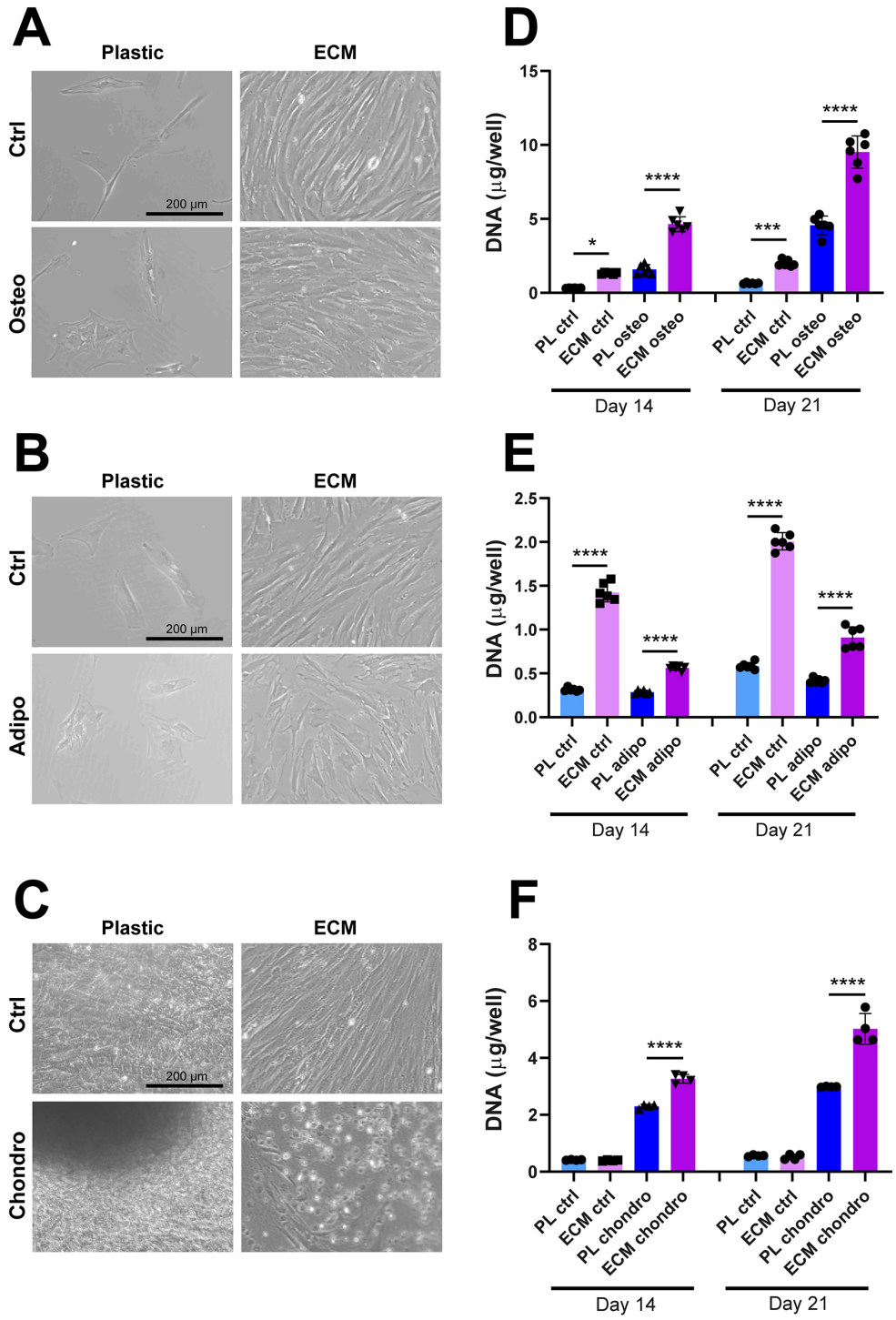

Fig. 1. Enhanced proliferation of human BMSCs on ECM layer in different culture conditions. (**A–C**) Representative images of enhanced cell growth after 5 days of culture on the ECM layer compared to standard tissue culture plastic in control, osteogenic, adipogenic and chondrogenic media. Scale bars: 200 µm. Group labels: Ctrl–control medium, Osteo–osteogenic differentiation medium, Adipo–adipogenic differentiation medium and Chondro–chondrogenic differentiation medium. (**D–F**) DNA content quantification of BMSC cultures on the ECM layer and tissue culture plastic during osteogenic (**D**), adipogenic (**E**) and chondrogenic (**F**) differentiation. Group labels: PL ctrl–plastic with control medium, ECM ctrl–ECM with control medium, PL osteo–plastic with osteogenic differentiation medium, ECM osteo–ECM with osteogenic differentiation medium, PL adipo–plastic with adipogenic differentiation medium, ECM adipo–ECM with adipogenic differentiation medium, PL chondro–plastic with chondrogenic differentiation medium, ECM chondro–ECM with chondrogenic differentiation medium. Data represents mean ± SD (n = 4–6). Statistically-significant differences between the groups were evaluated using two-way ANOVA, followed by Tukey's multiple comparison test, and are marked with: *$p < 0.05$; ***$p < 0.001$; ****$p < 0.0001$. BMSCs, bone marrow-derived MSCs; ECM, extracellular matrix.

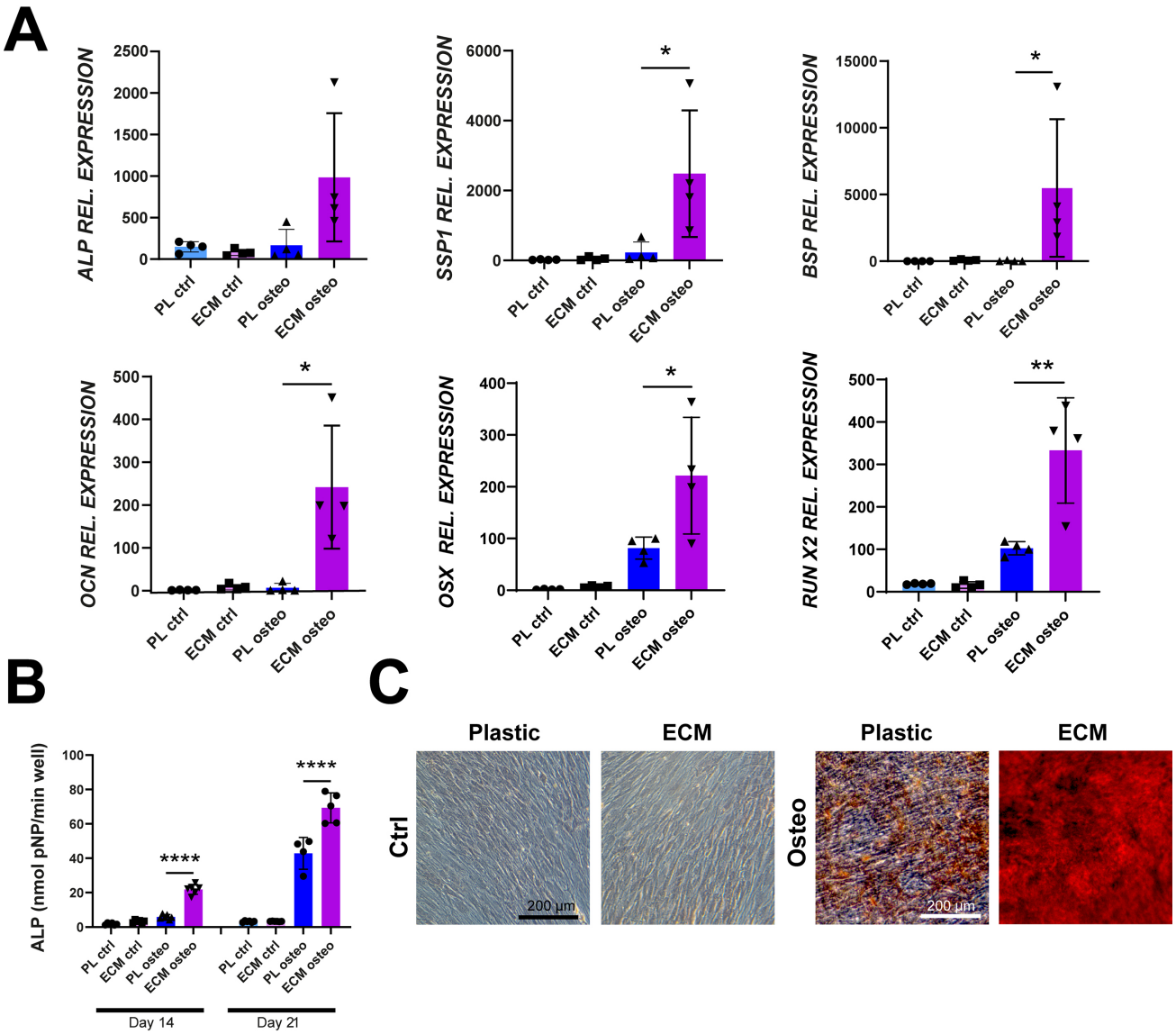

Fig. 2. Enhanced osteogenic differentiation of human BMSCs on ECM layer. (**A**) Relative gene expression levels of osteogenic markers alkaline phosphatase (ALP), osteopontin (SSP1), bone sialoprotein (BSP) osteocalcin (OCN), osterix (OSX) and runt related transcription factor 2 (RUNX2) after 21 days of culture. (**B**) ALP activity after 14 and 21 days of culture. (**A,B**) Group labels: PL ctrl–plastic with control medium, ECM ctrl–ECM with control medium, PL osteo–plastic with osteogenic differentiation medium, ECM osteo–ECM with osteogenic differentiation medium. Data represents mean ± SD (n = 4–6). Statistically-significant differences between the groups were evaluated using Kruskal–Wallis test, followed by Dunn's multiple comparison test (Panel **A**), or two-way ANOVA, followed by Tukey's multiple comparison test (Panel **B**), and are marked with: *$p < 0.05$; **$p < 0.01$; ****$p < 0.0001$. (**C**) Alizarin Red staining for mineral deposition (red deposits) after 42 days of culture. Representative images are shown (n = 3). Scale bars: 200 µm.

ference between the micromass cultures. Moreover, after 21 days of culture, we found a significant increase in GAG deposition by the BMSCs in chondrogenic differentiation medium on the ECM compared to tissue culture plastic (Fig. 4**B**). GAG deposition normalized to DNA content was not significantly different between the two groups (**Supplementary Fig. 2**). Histological staining of one randomly sampled micromass tissue per group was conducted to evaluate the matrix deposition pattern (Fig. 4**C,D**). The increase in GAG content corresponded with the Alcian blue histological staining, which showed a more uniform GAG deposition when human BMSCs were cultured on the ECM as compared to tissue culture plastic under chondrogenic induction (Fig. 4**C**). Furthermore, a more uniform collagen type II deposition could be observed in the micromass sample cultured for 21 days in differentiation medium on the ECM (Fig. 4**D**). Taken together, these data show an enhancement of chondrogenic differentiation of BMSCs on the ECM layer with no concomitant increase in hypertrophy marker expression.

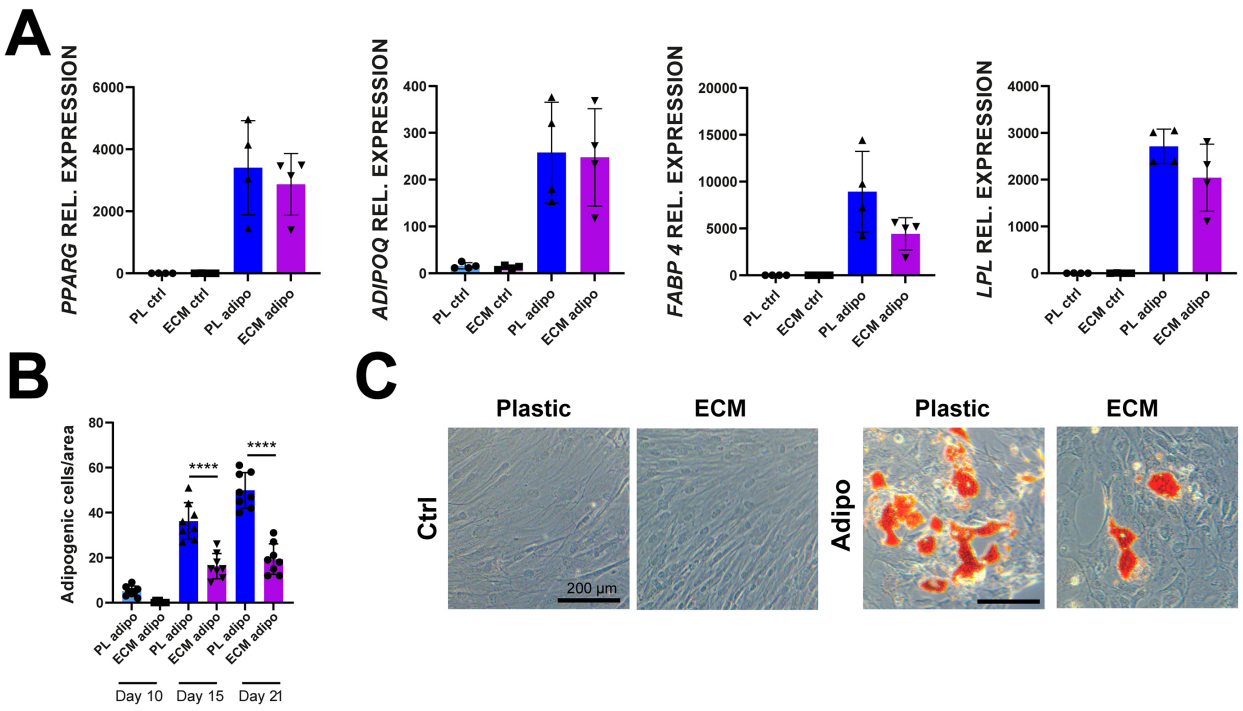

Fig. 3. Reduced adipocyte formation by human BMSCs on ECM layer. (**A**) Relative gene expression levels of adipogenic markers peroxisome proliferator activated receptor gamma (PPARG), adiponectin (ADIPOQ), fatty acid binding protein 4 (FABP4) and lipoprotein lipase (LPL) after 21 days of culture. (**B**) Adipocyte formation during 21 days of culture. (**A,B**) Group labels: PL ctrl–plastic with control medium, ECM ctrl–ECM with control medium, PL adipo–plastic with adipogenic differentiation medium, ECM adipo–ECM with adipogenic differentiation medium. Data represents mean ± SD (n = 4 or 8). Statistically-significant differences between the groups were evaluated using Kruskal–Wallis test, followed by Dunn's multiple comparison test (Panel **A**), or two-way ANOVA, followed by Tukey's multiple comparison test (Panel **B**), and are marked with: ****$p < 0.0001$. (**C**) Oil red O staining for lipid-laden adipocyte formation (red) after 21 days of culture. Representative images are shown (n = 3). Scale bars: 200 µm.

Cultivation on hiPSC-MP-ECM Modulates IL-6 Secretion by Differentiating Human BMSCs

To determine whether exposure to the hiPSC-MP ECM layer affects BMSC secretory activity, we evaluated secretion of IL-6 in supernatants of human BMSCs after 3 and 21 days of differentiation on the ECM layer and on tissue culture plastic (Fig. 5). After 3 days of culture, IL-6 concentration was the highest in monolayer and micromass cultures growing in control medium, with no significant differences between the ECM layer and tissue culture plastic (Fig. 5). BMSCs in osteogenic and adipogenic differentiation media in monolayer cultures showed comparable low IL-6 concentrations on ECM layer and tissue culture plastic. In contrast, BMSC micromass cultures in chondrogenic differentiation medium showed a significant increase in IL-6 concentration on the ECM layer compared to tissue culture plastic. After 21 days of culture, IL-6 concentration of monolayer culture groups in control medium was lower compared to the earlier timepoint with no significant difference between the ECM layer and tissue culture plastic. In contrast, BMSC micromass cultures in control medium exhibited a significantly higher IL-6 concentration on tissue culture plastic as compared to ECM layer after 21 days. IL-6 concentration was also significantly higher in monolayer cultures in osteogenic differentiation medium on tissue culture plastic compared to culture on ECM layer, whereas concentrations of IL-6 in adipogenic and chondrogenic differentiation media were low on both culture surfaces. Taken together, our data indicate that cultivation on the ECM layer modulates the release of IL-6 compared with tissue culture plastic, and the cell secretory responses depend on culture conditions and duration of culture.

Discussion

Engineered ECMs are biological scaffolds that mimic the complex structure and signaling of native tissues and are therefore intensely investigated for bone and osteochondral tissue engineering and regeneration (Benders *et al*., 2013; Förster *et al*., 2012; Zhang *et al*., 2016). ECM engineering utilizing primary MSCs faces challenges due to donor variability, limited cell numbers, limited cell expansion potential and loss of regenerative capacity after *in vitro* expansion. In contrast, hiPSCs represent a scalable source for production of youthful human progenitor cells such as hiPSC-MPs and bioactive tissue components, thus supporting eventual clinical translation. In our previous study, we engineered ECM from hiPSC-MPs and found that it strongly enhanced the osteogenic capacity of primary hu-

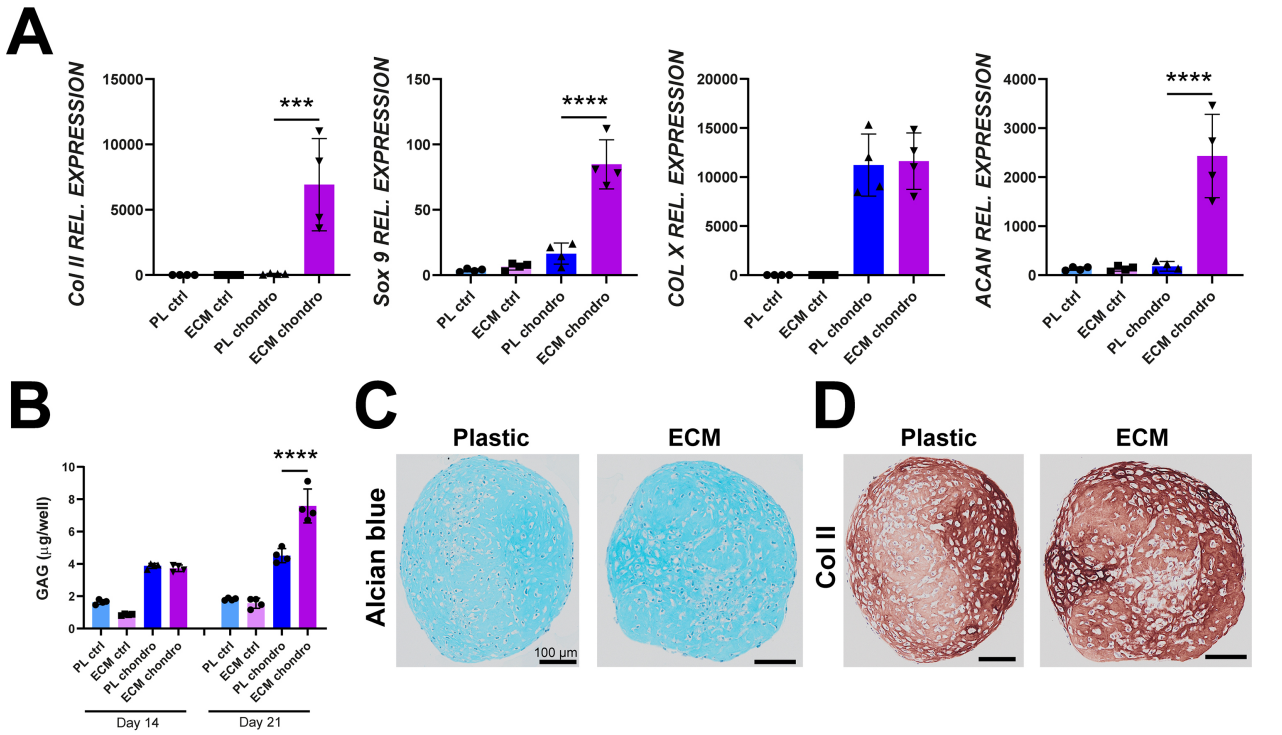

Fig. 4. Enhanced chondrogenic differentiation of human BMSCs on ECM layer. (**A**) Relative gene expression levels of chondrogenic markers collagen type II (COL II), SRY-box 9 (Sox9), collagen type X (COL X) and aggrecan (ACAN) after 21 days of culture. (**B**) GAG deposition after 21 days of culture. (**A,B**) Group labels: PL ctrl–plastic with control medium, ECM ctrl–ECM with control medium, PL chondro–plastic with chondrogenic differentiation medium, ECM chondro–ECM with chondrogenic differentiation medium. Data represents mean ± SD (n = 4). Statistically-significant differences between the groups were evaluated using Kruskal–Wallis test, followed by Dunn's multiple comparison test (Panel **A**), or two-way ANOVA, followed by Tukey's multiple comparison test (Panel **B**), and are marked with: ***$p < 0.001$; ****$p < 0.0001$. (**C**) Alcian blue staining for GAG deposition (blue) after 21 days of culture. (**D**) Immunohistochemical staining for collagen type II deposition (brown) after 21 days of culture. (**C,D**) Staining of one randomly sampled micromass tissue per group is shown. Scale bars: 100 µm.

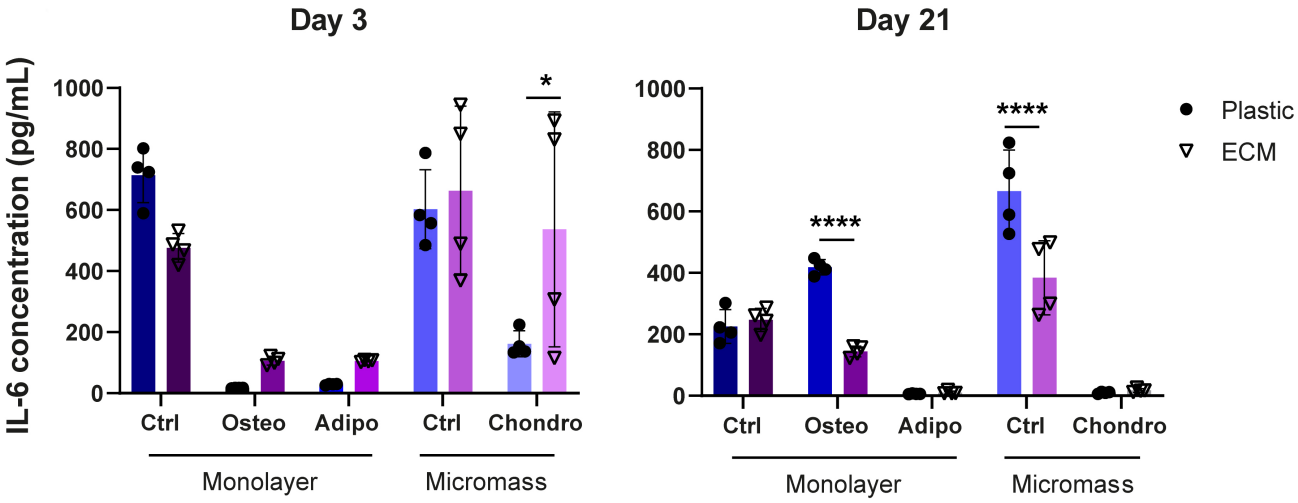

Fig. 5. Effects of culture on ECM layer on IL-6 secretion during BMSC differentiation. Concentrations of IL-6 after 3 and 21 days of culture were determined by ELISA. Group labels monolayer cultures: Ctrl–plastic or ECM with control medium, Osteo–plastic or ECM with osteogenic differentiation medium, Adipo–plastic or ECM with adipogenic differentiation medium. Group labels micromass cultures: Ctrl–plastic or ECM with control medium, Chondro–plastic or ECM with chondrogenic differentiation medium. Statistically significant differences between the groups were evaluated using two-way ANOVA, followed by Tukey's multiple comparison test, and the differences between ECM and plastic groups are marked with: *$p < 0.05$; ****$p < 0.0001$.

man BMSCs from young adult- and aged donors in two- and three-dimensional culture models (Hanetseder *et al*., 2023). Therefore, in the current study, we investigated (using cells from the same young adult donor) whether culture on hiPSC-MP-ECM affects the BMSC trilineage differentiation and associated secretory activity compared to BMSCs cultured on standard tissue culture plastic. We found that the hiPSC-MP-ECM strongly enhanced cell growth in control and differentiation culture conditions. Furthermore, BMSC culture on the ECM enhanced osteogenic and chondrogenic differentiation, while reducing adipocyte formation. BMSC culture on hiPSC-MP-ECM layer also significantly affected the secretion of IL-6 after 3 and 21 days of differentiation, pointing to the importance of the ECM microenvironment for BMSC trophic activity.

The ability of MSC-derived ECMs to significantly enhance cell expansion in growth media compared to standard tissue culture plastic has already been shown in several studies (Chen *et al*., 2007; He and Pei, 2013; Lai *et al*., 2010; Ng *et al*., 2014; Yang *et al*., 2018). In line with these studies and our prior work (Hanetseder *et al*., 2023), we found that hiPSC-MP-ECM enhanced BMSC proliferation in monolayer cultures also in control medium. Furthermore, enhanced BMSCs proliferation was noted in all three differentiation conditions, i.e., in osteogenic and adipogenic differentiation media in monolayer cultures and in chondrogenic differentiation medium in micromass cultures. To our knowledge, our study is the first to find enhanced cell proliferation during osteogenic-, chondrogenic- and adipogenic differentiation on the same cell-derived ECM layer compared to standard tissue culture plastic. Ng *et al*. also showed that late-passage adult MSC properties were significantly improved on fetal MSCs-derived ECM, including cell proliferation, stemness and osteogenic, adipogenic and chondrogenic differentiation compared to tissue culture plastic. Together, these studies and our work suggest that ECMs from biologically-young cells could be a promising substrate to improve *ex vivo* expansion of autologous MSCs for clinical applications (Chen *et al*., 2007; Ng *et al*., 2014). Furthermore, our current study indicates that differentiation of MSCs on the ECM presents an additional advantage, as it further increases the yield of differentiating cells.

ECM in the current study was generated using the same procedure as in our previous study, which confirmed the maintenance of collagen type I, collagen type IV, laminin and fibronectin in the ECM after the decellularization procedure (Hanetseder *et al*., 2023). It was previously shown that individual ECM proteins such as collagens, fibronectin and laminin have a proliferative effect on BMSCs (Becerra-Bayona *et al*., 2012; Kihara *et al*., 2006; Linsley *et al*., 2013; Mizuno *et al*., 2000; Nieto-Nicolau *et al*., 2020; Salasznyk *et al*., 2004). Furthermore, we and others found that the cultivation on engineered ECM resulted in stronger enhancement of adult BMSC growth compared to single protein substrates (Hanetseder *et al*., 2023; Ng *et al*., 2014). It remains to be determined whether this effect is mainly due to the synergistic signaling activity of individual ECM components, or whether this is also affected by the mechanical properties of the ECM mimicking the native tissue (Marinkovic *et al*., 2020). Interestingly, prior studies showed that despite unique matrisome signatures of individual ECMs derived from BMSCs, adipose derived MSC or neonatal dermal fibroblasts, the overall stimulatory effects on MSC proliferation were comparable (Prewitz *et al*., 2013; Ragelle *et al*., 2017).

Engineered ECMs were previously found to enhance osteogenic, chondrogenic and adipogenic differentiation in various study setups (Ang *et al*., 2014; Carvalho *et al*., 2019; Cheng *et al*., 2009; Jeon *et al*., 2018; Lu *et al*., 2011). With regards to osteogenic differentiation, ECM layers engineered from young adult human BMSCs enhanced alkaline phosphatase activity, gene expression of *Col1A1*, *RUNX 2* and *ALP* and mineralization of human BMSCs (Carvalho *et al*., 2019). We have already shown in our previous study that both hiPSC-MP-ECM layer and silk scaffold coating increased osteogenic gene expression, bone matrix proteins deposition and mineralization of BMSCs from young adult and especially from aged donors (Hanetseder *et al*., 2023). In line with these findings, enhancement of young adult BMSC osteogenic differentiation on the ECM layer was also observed in the current study, using the same donor cells in an independent experiment. We noted significantly increased ALP activity after 14 and 21 days, that could be attributed to increased cell proliferation, as well as significantly increased osteogenic gene expression after 21 days and matrix mineralization after 42 days. While some differences in ALP activity responses of young adult BMSCs derived from the same donor were noted between our two studies, the overall ALP activity levels reached were similar between the studies. These differences might be attributed to inter-experimental variation, as it is known that increase in ALP activity is an early marker of osteogenic differentiation, which changes dynamically with the progress of differentiation (Malaval *et al*., 1994). Significant increase in expression of transcription factors *RUNX2* and OSX in osteogenic conditions, further induced by the ECM, is in line with their roles in osteogenic lineage induction and osteoblast differentiation (Chan *et al*., 2021). Interestingly, RUNX2 expression was significantly decreased in adipogenic cultures on the ECM, suggesting the ECM acts on adipogenic/osteogenic differentiation regulatory network (Rauch *et al*., 2019).

Furthermore, ECM layers derived from osteogenic- or adipogenic-induced MSCs were shown to specifically enhance the corresponding lineage in re-seeded MSCs through integrated structural and regulatory proteins (Ang *et al*., 2014; Carvalho *et al*., 2019; Jeon *et al*., 2018). Ang *et al*. showed that collagen type IV is one of the major components of basement membranes, which provides

structural support for mature lipid-laden adipocytes (Ang *et al*., 2014). They also indicated that under macromolecular crowding conditions, adipogenic-induced human BMSCs shifted from collagen type I toward collagen type IV production and reduced fibronectin deposition in their ECM. In our previous study, we found adipocyte formation in osteogenic cultures of aged donor BMSCs on tissue culture plastic. However, no adipocytes were noted on hiPSC-MP-derived ECM (Hanetseder *et al*., 2023). We were therefore interested in how the ECM would affect BMSC induction into adipogenic lineage. Interestingly, we found a comparable expression of genes for adipogenic master regulator *PPARG* and adiponectin (*ADIPOQ*), a hormone which is thought to be active further downstream in the adipocytokine signaling pathway (Menssen *et al*., 2011) in BMSCs cultured on the ECM as compared to tissue culture plastic. Genes coding for fatty acid-binding protein 4, implicated in early adipogenesis, and lipoprotein lipase (*LPL*) (Menssen *et al*., 2011) exhibited a trend of lower expression in BMSCs cultured on the ECM layer compared to tissue culture plastic. However, a significant reduction in the formation of mature, lipid-laden adipocytes was found on the ECM layer compared to tissue culture plastic in adipogenic differentiation medium. It was shown previously that osteogenesis and adipogenesis are inversely related processes, where osteogenesis depends on commissioning of a network of MSC transcription factors that act as repressors of adipogenesis (Rauch *et al*., 2019; Suo *et al*., 2022). In line with this, our data suggest that the hiPSC-MP-ECM signals a shift in adult BMSC differentiation balance from adipogenic to osteogenic differentiation.

In prior studies, the stimulatory effect of cell-generated ECM on chondrogenic differentiation was demonstrated for hybrid ECM scaffolds and scaffolds composed fully of ECM (Cheng *et al*., 2009; Jin *et al*., 2007; Lu *et al*., 2011; Tang *et al*., 2013, 2014; Yuan *et al*., 2013). These scaffolds were shown to contain ECM components that activate integrin signaling as well as pro-chondrogenic growth factors that are retained in the matrix after chemical decellularization (Benders *et al*., 2013; Chiang *et al*., 2021). Furthermore, cell-derived ECM layers were shown to promote the maintenance of a primary chondrocyte phenotype during expansion. For instance, Pei *et al*. showed that porcine chondrocytes exhibited a higher collagen type II gene expression after expansion on a synovium stem cell-derived ECM compared to tissue culture plastic (Pei and He, 2012), and Yang *et al*. demonstrated that hBMSC-ECM delayed dedifferentiation of expanded chondrocytes compared to tissue culture plastic (Yang *et al*., 2018). In both studies, the harvested chondrocytes showed an improved redifferentiation ability when placed in a micromass culture system compared to chondrocytes expanded on standard tissue culture plastic (Pei and He, 2012; Yang *et al*., 2018). To our knowledge, the potential of cell-derived ECM to enhance chondrogenic differentiation of adult human BMSCs in micromass culture has not been previously assessed. We found increased gene expression of chondrogenic markers, including the master regulator SOX9, as well as collagen type II and aggrecan, both markers of the mature chondrocyte phenotype (Mwale *et al*., 2006) in BMSCs cultured on the ECM compared to tissue culture plastic. In contrast, no increase was found in collagen type X gene expression, suggesting that the ECM does not facilitate BMSC differentiation towards hypertrophy compared to tissue culture plastic (Mueller and Tuan, 2008; Yang *et al*., 2019). Enhanced expression of cartilaginous specific gene markers in our BMSC micromass cultures on the ECM layer also correlated with increased and more uniform collagen type II and GAG deposition, as found in previous studies in pellet-micromass culture model (Lu *et al*., 2011; Yang *et al*., 2018). However, the full impact of ECM on chondrogenic induction of BMSCs and the potential for stable cartilage formation vs. induction of endochondral ossification pathway needs to be further evaluated.

Finally, we aimed to assess how BMSC secretory activity is affected by differentiation on the ECM layer. We focused on evaluating the secretion of IL-6, a cytokine with pleiotropic roles in the regulation of the immune system (Dorronsoro *et al*., 2020). In the context of osteogenic differentiation, it was previously reported that IL-6 secretion is high in undifferentiated BMSCs, whereas it decreases during BMSC differentiation (Pricola *et al*., 2009). It was also suggested that IL-6 inhibited BMSC differentiation (Bian *et al*., 2010; Pricola *et al*., 2009). In the context of cartilage repair, increased levels of IL-6 were shown to promote the anabolic metabolism of chondrocytes, and to be supportive for neocartilage formation (Tsuchida *et al*., 2012). In our study, IL-6 secretion was highest in BMSCs cultured in control medium in monolayer and micromass cultures. In contrast to a prior report (Pricola *et al*., 2009), we found a significant increase in IL-6 release by BMSCs in the later stage of osteogenic differentiation when cells where cultured on standard tissue culture plastic compared to the ECM layer. It was previously shown that growth plate- but not articular cartilage-derived ECM induced production of IL-6 and TNF, both of which have a pro-osteogenic role (Glass *et al*., 2011; Huang *et al*., 2018; Kurozumi *et al*., 2019). In chondrogenic micromass cultures, IL-6 secretion was also significantly enhanced by the ECM layer at an earlier point of induction, coinciding with enhanced cell proliferation. At the later stage of chondrogenic differentiation, IL-6 secretion was practically undetectable on both culture surfaces. Together, our data suggest that the microenvironment provided by the ECM layer as well as the differentiation medium signals affect the BMSC secretory activity. Modulation of BMSC secretory activity thus needs to be considered within the context of BMSC-based regenerative therapies utilizing engineered ECM.

The results presented here are the first step in evaluating the potential of hiPSC-MP-derived ECM to modulate

trilineage differentiation of BMSCs for potential applications in bone and osteochondral regenerative therapies. In future studies, the key ECM components responsible for enhancing BMSC proliferation and modulating trilineage differentiation, their stability, and the molecular mechanisms will need to be elucidated. Also, it remains to be determined whether BMSC donor age affects the cells' sensitivity to the signals provided by hiPSC-MP-derived ECM, since we only tested the effects of hiPSC-MP-ECM on BMSCs derived from a young adult donor, which exhibited a strong differentiation potential. Decline in osteogenic differentiation capability has been found in BMSCs from aged donors, and it would be interesting to evaluate whether the shift in differentiation potential found in the young donor BMSCs could also be achieved for chronologically aged BMSCs.

Conclusions

In conclusion, we have shown that osteogenic and chondrogenic differentiation of young adult human BMSCs can be strongly enhanced by culturing them on an ECM layer engineered *in vitro* from hiPSC-MPs. We have also shown that hiPSC-MP ECM enhanced cell growth in different culture conditions while reducing lipid-laden adipocyte formation. However, this study has not undertaken a quantitative analysis of the ECM components and their role in stimulatory actions. It remains to be established which particular components, along with the structure and mechanical properties of the ECM, are contributing to the stimulatory effects on BMSC growth and differentiation. With hiPSCs representing a potentially unlimited and scalable human cell source, developing tissue engineering strategies employing hiPSC-engineered ECM could be a feasible and attractive approach for osteochondral defect repair.

List of Abbreviations

BMSCs, bone marrow-derived MSCs; ECM, extracellular matrix; MSCs, mesenchymal stromal cells; 3D, three-dimensional; hiPSC-MPs, human MSC-like progenitors; KO-DMEM, KnockOut Dulbecco's modified Eagle's medium; FBS, fetal bovine serum; P/S, penicillin-streptomycin; b-FGF, basic fibroblast growth factor; DMEM-HG, Dulbecco's modified Eagle's medium high glucose; A2P, ascorbic acid 2-phosphate; PBS, phosphate-buffered saline; TGF-β3, transforming growth factor-β3; ALP, alkaline phosphatase; pNPP, para-Nitrophenylphosphate; GAG, glycosaminoglycans; PPARG, peroxisome proliferator activated receptor gamma; ADIPOQ, adiponectin; FABP4, fatty acid binding protein 4; LPL, lipoprotein lipase; COL2A1, Collagen type II; ACAN, Aggrecan; COL10A1, Collagen type X; Sox9, SRY-box 9; RUNX2, runt related transcription factor 2; GAPDH, glyceraldehyde 3-phosphate dehydrogenase; IL-6, interleukin 6; SSP1, osteopontin; BSP, bone sialoprotein; OCN, osteocalcin; OSX, osterix.

Availability of Data and Materials

All datasets and materials gathered are incuded in the published manuscript.

Author Contributions

Conceptualization and study design, DH, HR and DMP; Investigation, methodology and visualization, DH and BS; Formal analysis, DH, HR and DMP; Writing—original draft, DH and DMP; Writing—review & editing, DH, HR, BS and DMP; Project administration, DMP; Project supervision, HR and DMP. All authors were informed about each step of manuscript processing and have read and agreed to the published version of the manuscript.

Ethics Approval and Consent to Participate

Not applicable.

Acknowledgments

We would like to thank our colleagues from Ludwig Boltzmann Institute for Traumatology for their suggestions and support of the project, especially Vanessa Goeschl for her help with cell culture. We would like to thank Regina Brunauer and Simon Sperger for their suggestions with manuscript writing. We further thank the New York Stem Cell Foundation Research Institute for providing the human induced pluripotent stem cell line 1013A and its mesenchymal progenitors. The graphical abstract was created with the online tool BioRender.com.

Funding

This work has received funding from the European Union's Horizon 2020 research and innovation programme under the Marie Sklodowska-Curie actions (grant agreement No. 657716) and Transforming European Industry call H2020-NMBP-TR-IND-2020 (grant agreement No. 953134), as well as by the FFG Industrienahe Dissertation program (grant agreement No. 867803) and the FFG Production of the Future program (grant agreement No. 877452).

Conflict of Interest

The authors declare no conflict of interest.

Supplementary Material

Supplementary material associated with this article can be found, in the online version, at https://doi.org/10.22203/eCM.v047a08.

References

Ang XM, Lee MHC, Blocki A, Chen C, Ong LLS, Asada HH, Sheppard A, Raghunath M (2014) Macromolecular crowding amplifies adipogenesis of human bone marrow-derived mesenchymal stem cells by enhancing the

pro-adipogenic microenvironment. Tissue Engineering. Part a 20: 966-981. DOI: 10.1089/ten.TEA.2013.0337.

Arnott JA, Lambi AG, Mundy C, Hendesi H, Pixley RA, Owen TA, Safadi FF, Popoff SN (2011) The role of connective tissue growth factor (CTGF/CCN2) in skeletogenesis. Critical Reviews in Eukaryotic Gene Expression 21: 43-69. DOI: 10.1615/critreveukargeneexpr.v21.i1.40.

Assunção M, Dehghan-Baniani D, Yiu CHK, Später T, Beyer S, Blocki A (2020) Cell-Derived Extracellular Matrix for Tissue Engineering and Regenerative Medicine. Frontiers in Bioengineering and Biotechnology 8: 602009 DOI: 10.3389/fbioe.2020.602009.

Becerra-Bayona S, Guiza-Arguello V, Qu X, Munoz-Pinto DJ, Hahn MS (2012) Influence of select extracellular matrix proteins on mesenchymal stem cell osteogenic commitment in three-dimensional contexts. Acta Biomaterialia 8: 4397-4404. DOI: 10.1016/j.actbio.2012.07.048.

Benders KEM, van Weeren PR, Badylak SF, Saris DBF, Dhert WJA, Malda J (2013) Extracellular matrix scaffolds for cartilage and bone regeneration. Trends in Biotechnology 31: 169-176. DOI: 10.1016/j.tibtech.2012.12.004.

Bian ZY, Fan QM, Li G, Xu WT, Tang TT (2010) Human mesenchymal stem cells promote growth of osteosarcoma: involvement of interleukin-6 in the interaction between human mesenchymal stem cells and Saos-2. Cancer Science 101: 2554-2560. DOI: 10.1111/j.1349-7006.2010.01731.x.

Bianco P, Kuznetsov SA, Riminucci M, Gehron Robey P (2006) Postnatal skeletal stem cells. Methods in Enzymology 419: 117-148. DOI: 10.1016/S0076-6879(06)19006-0.

Bruder SP, Jaiswal N, Haynesworth SE (1997) Growth kinetics, self-renewal, and the osteogenic potential of purified human mesenchymal stem cells during extensive subcultivation and following cryopreservation. Journal of Cellular Biochemistry 64: 278-294. DOI: 10.1002/(sici)1097-4644(199702)64:2<278::aid-jcb11>3.0.co;2-f.

Carvalho MS, Silva JC, Cabral JMS, da Silva CL, Vashishth D (2019) Cultured cell-derived extracellular matrices to enhance the osteogenic differentiation and angiogenic properties of human mesenchymal stem/stromal cells. Journal of Tissue Engineering and Regenerative Medicine 13: 1544-1558. DOI: 10.1002/term.2907.

Chan WCW, Tan Z, To MKT, Chan D (2021) Regulation and Role of Transcription Factors in Osteogenesis. International Journal of Molecular Sciences 22: 5445 DOI: 10.3390/ijms22115445.

Chen XD, Dusevich V, Feng JQ, Manolagas SC, Jilka RL (2007) Extracellular matrix made by bone marrow cells facilitates expansion of marrow-derived mesenchymal progenitor cells and prevents their differentiation into osteoblasts. Journal of Bone and Mineral Research: the Official Journal of the American Society for Bone and Mineral Research 22: 1943-1956. DOI: 10.1359/jbmr.070725.

Cheng HW, Tsui YK, Cheung KMC, Chan D, Chan BP (2009) Decellularization of chondrocyte-encapsulated collagen microspheres: a three-dimensional model to study the effects of acellular matrix on stem cell fate. Tissue Engineering. Part C, Methods 15: 697-706. DOI: 10.1089/ten.TEC.2008.0635.

Chiang CE, Fang YQ, Ho CT, Assunção M, Lin SJ, Wang YC, Blocki A, Huang CC (2021) Bioactive Decellularized Extracellular Matrix Derived from 3D Stem Cell Spheroids under Macromolecular Crowding Serves as a Scaffold for Tissue Engineering. Advanced Healthcare Materials 10: e2100024 DOI: 10.1002/adhm.202100024.

Coleman CM, Vaughan EE, Browe DC, Mooney E, Howard L, Barry F (2013) Growth differentiation factor-5 enhances in vitro mesenchymal stromal cell chondrogenesis and hypertrophy. Stem Cells and Development 22: 1968-1976. DOI: 10.1089/scd.2012.0282.

de Peppo GM, Marcos-Campos I, Kahler DJ, Alsalman D, Shang L, Vunjak-Novakovic G, Marolt D (2013) Engineering bone tissue substitutes from human induced pluripotent stem cells. Proceedings of the National Academy of Sciences of the United States of America 110: 8680-8685. DOI: 10.1073/pnas.1301190110.

Dominici M, Le Blanc K, Mueller I, Slaper-Cortenbach I, Marini F, Krause D, Deans R, Keating A, Prockop D, Horwitz E (2006) Minimal criteria for defining multipotent mesenchymal stromal cells. The International Society for Cellular Therapy position statement. Cytotherapy 8: 315-317. DOI: 10.1080/14653240600855905.

Dorronsoro A, Lang V, Ferrin I, Fernández-Rueda J, Zabaleta L, Pérez-Ruiz E, Sepúlveda P, Trigueros C (2020) Intracellular role of IL-6 in mesenchymal stromal cell immunosuppression and proliferation. Scientific Reports 10: 21853 DOI: 10.1038/s41598-020-78864-4.

Fernandez-Rebollo E, Franzen J, Goetzke R, Hollmann J, Ostrowska A, Oliverio M, Sieben T, Rath B, Kornfeld JW, Wagner W (2020) Senescence-Associated Metabolomic Phenotype in Primary and iPSC-Derived Mesenchymal Stromal Cells. Stem Cell Reports 14: 201-209. DOI: 10.1016/j.stemcr.2019.12.012.

Fitzpatrick LE, McDevitt TC (2015) Cell-derived matrices for tissue engineering and regenerative medicine applications. Biomaterials Science 3: 12-24. DOI: 10.1039/C4BM00246F.

Förster Y, Rentsch C, Schneiders W, Bernhardt R, Simon JC, Worch H, Rammelt S (2012) Surface modification of implants in long bone. Biomatter 2: 149-157. DOI: 10.4161/biom.21563.

Freytes DO, Wan LQ, Vunjak-Novakovic G (2009) Geometry and force control of cell function. Journal of Cellular Biochemistry 108: 1047-1058. DOI: 10.1002/jcb.22355.

Frobel J, Hemeda H, Lenz M, Abagnale G, Joussen S, Denecke B, Sarić T, Zenke M, Wagner W (2014) Epi-

genetic rejuvenation of mesenchymal stromal cells derived from induced pluripotent stem cells. Stem Cell Reports 3: 414-422. DOI: 10.1016/j.stemcr.2014.07.003.

Glass GE, Chan JK, Freidin A, Feldmann M, Horwood NJ, Nanchahal J (2011) TNF-alpha promotes fracture repair by augmenting the recruitment and differentiation of muscle-derived stromal cells. Proceedings of the National Academy of Sciences of the United States of America 108: 1585-1590. DOI: 10.1073/pnas.1018501108.

Gresham RCH, Bahney CS, Leach JK (2020) Growth factor delivery using extracellular matrix-mimicking substrates for musculoskeletal tissue engineering and repair. Bioactive Materials 6: 1945-1956. DOI: 10.1016/j.bioactmat.2020.12.012.

Hanetseder D, Levstek T, Teuschl-Woller AH, Frank JK, Schaedl B, Redl H, Marolt Presen D (2023) Engineering of extracellular matrix from human iPSC-mesenchymal progenitors to enhance osteogenic capacity of human bone marrow stromal cells independent of their age. Frontiers in Bioengineering and Biotechnology 11: 1214019 DOI: 10.3389/fbioe.2023.1214019.

He F, Pei M (2013) Extracellular matrix enhances differentiation of adipose stem cells from infrapatellar fat pad toward chondrogenesis. Journal of Tissue Engineering and Regenerative Medicine 7: 73-84. DOI: 10.1002/term.505.

Huang RL, Sun Y, Ho CK, Liu K, Tang QQ, Xie Y, Li Q (2018) IL-6 potentiates BMP-2-induced osteogenesis and adipogenesis via two different BMPR1A-mediated pathways. Cell Death & Disease 9: 144 DOI: 10.1038/s41419-017-0126-0.

Hynes RO, Naba A (2012) Overview of the matrisome–an inventory of extracellular matrix constituents and functions. Cold Spring Harbor Perspectives in Biology 4: a004903 DOI: 10.1101/cshperspect.a004903.

Jeon J, Lee MS, Yang HS (2018) Differentiated osteoblasts derived decellularized extracellular matrix to promote osteogenic differentiation. Biomaterials Research 22: 4 DOI: 10.1186/s40824-018-0115-0.

Jin CZ, Park SR, Choi BH, Park K, Min BH (2007) In vivo cartilage tissue engineering using a cell-derived extracellular matrix scaffold. Artificial Organs 31: 183-192. DOI: 10.1111/j.1525-1594.2007.00363.x.

Kern S, Eichler H, Stoeve J, Klüter H, Bieback K (2006) Comparative analysis of mesenchymal stem cells from bone marrow, umbilical cord blood, or adipose tissue. Stem Cells (Dayton, Ohio) 24: 1294-1301. DOI: 10.1634/stemcells.2005-0342.

Kihara T, Hirose M, Oshima A, Ohgushi H (2006) Exogenous type I collagen facilitates osteogenic differentiation and acts as a substrate for mineralization of rat marrow mesenchymal stem cells in vitro. Biochemical and Biophysical Research Communications 341: 1029-1035. DOI: 10.1016/j.bbrc.2006.01.059.

Krampera M, Le Blanc K (2021) Mesenchymal stromal cells: Putative microenvironmental modulators become cell therapy. Cell Stem Cell 28: 1708-1725. DOI: 10.1016/j.stem.2021.09.006.

Kurozumi A, Nakano K, Yamagata K, Okada Y, Nakayamada S, Tanaka Y (2019) IL-6 and sIL-6R induces STAT3-dependent differentiation of human VSMCs into osteoblast-like cells through JMJD2B-mediated histone demethylation of RUNX2. Bone 124: 53-61. DOI: 10.1016/j.bone.2019.04.006.

Kuznetsov SA, Hailu-Lazmi A, Cherman N, de Castro LF, Robey PG, Gorodetsky R (2019) In Vivo Formation of Stable Hyaline Cartilage by Naïve Human Bone Marrow Stromal Cells with Modified Fibrin Microbeads. Stem Cells Translational Medicine 8: 586-592. DOI: 10.1002/sctm.18-0129.

Lai Y, Sun Y, Skinner CM, Son EL, Lu Z, Tuan RS, Jilka RL, Ling J, Chen XD (2010) Reconstitution of marrow-derived extracellular matrix ex vivo: a robust culture system for expanding large-scale highly functional human mesenchymal stem cells. Stem Cells and Development 19: 1095-1107. DOI: 10.1089/scd.2009.0217.

Lapasset L, Milhavet O, Prieur A, Besnard E, Babled A, Aït-Hamou N, Leschik J, Pellestor F, Ramirez JM, De Vos J, Lehmann S, Lemaitre JM (2011) Rejuvenating senescent and centenarian human cells by reprogramming through the pluripotent state. Genes & Development 25: 2248-2253. DOI: 10.1101/gad.173922.111.

Lian Q, Zhang Y, Zhang J, Zhang HK, Wu X, Zhang Y, Lam FFY, Kang S, Xia JC, Lai WH, Au KW, Chow YY, Siu CW, Lee CN, Tse HF (2010) Functional mesenchymal stem cells derived from human induced pluripotent stem cells attenuate limb ischemia in mice. Circulation 121: 1113-1123. DOI: 10.1161/CIRCULATIONAHA.109.898312.

Lin H, Yang G, Tan J, Tuan RS (2012) Influence of decellularized matrix derived from human mesenchymal stem cells on their proliferation, migration and multi-lineage differentiation potential. Biomaterials 33: 4480-4489. DOI: 10.1016/j.biomaterials.2012.03.012.

Linsley C, Wu B, Tawil B (2013) The effect of fibrinogen, collagen type I, and fibronectin on mesenchymal stem cell growth and differentiation into osteoblasts. Tissue Engineering. Part a 19: 1416-1423. DOI: 10.1089/ten.TEA.2012.0523.

Lu H, Hoshiba T, Kawazoe N, Koda I, Song M, Chen G (2011) Cultured cell-derived extracellular matrix scaffolds for tissue engineering. Biomaterials 32: 9658-9666. DOI: 10.1016/j.biomaterials.2011.08.091.

Malaval L, Modrowski D, Gupta AK, Aubin JE (1994) Cellular expression of bone-related proteins during in vitro osteogenesis in rat bone marrow stromal cell cultures. Journal of Cellular Physiology 158: 555-572. DOI: 10.1002/jcp.1041580322.

Mariman ECM, Wang P (2010) Adipocyte extracellular matrix composition, dynamics and role in obesity. Cellular and Molecular Life Sciences: CMLS 67: 1277-1292.

DOI: 10.1007/s00018-010-0263-4.

Marinkovic M, Tran ON, Block TJ, Rakian R, Gonzalez AO, Dean DD, Yeh CK, Chen XD (2020) Native extracellular matrix, synthesized ex vivo by bone marrow or adipose stromal cells, faithfully directs mesenchymal stem cell differentiation. Matrix Biology Plus 8: 100044 DOI: 10.1016/j.mbplus.2020.100044.

Marolt Presen D, Traweger A, Gimona M, Redl H (2019) Mesenchymal Stromal Cell-Based Bone Regeneration Therapies: From Cell Transplantation and Tissue Engineering to Therapeutic Secretomes and Extracellular Vesicles. Frontiers in Bioengineering and Biotechnology 7: 352 DOI: 10.3389/fbioe.2019.00352.

McKee TJ, Perlman G, Morris M, Komarova SV (2019) Extracellular matrix composition of connective tissues: a systematic review and meta-analysis. Scientific Reports 9: 10542 DOI: 10.1038/s41598-019-46896-0.

Mensing N, Gasse H, Hambruch N, Haeger JD, Pfarrer C, Staszyk C (2011) Isolation and characterization of multipotent mesenchymal stromal cells from the gingiva and the periodontal ligament of the horse. BMC Veterinary Research 7: 42 DOI: 10.1186/1746-6148-7-42.

Menssen A, Häupl T, Sittinger M, Delorme B, Charbord P, Ringe J (2011) Differential gene expression profiling of human bone marrow-derived mesenchymal stem cells during adipogenic development. BMC Genomics 12: 461 DOI: 10.1186/1471-2164-12-461.

Mizuno M, Fujisawa R, Kuboki Y (2000) Type I collagen-induced osteoblastic differentiation of bone-marrow cells mediated by collagen-alpha2beta1 integrin interaction. Journal of Cellular Physiology 184: 207-213. DOI: 10.1002/1097-4652(200008)184:2<207::AID-JCP8>3.0.CO;2-U.

Mueller MB, Tuan RS (2008) Functional characterization of hypertrophy in chondrogenesis of human mesenchymal stem cells. Arthritis and Rheumatism 58: 1377-1388. DOI: 10.1002/art.23370.

Murphy MB, Moncivais K, Caplan AI (2013) Mesenchymal stem cells: environmentally responsive therapeutics for regenerative medicine. Experimental & Molecular Medicine 45: e54 DOI: 10.1038/emm.2013.94.

Mwale F, Stachura D, Roughley P, Antoniou J (2006) Limitations of using aggrecan and type X collagen as markers of chondrogenesis in mesenchymal stem cell differentiation. Journal of Orthopaedic Research: Official Publication of the Orthopaedic Research Society 24: 1791-1798. DOI: 10.1002/jor.20200.

Narayanan K, Kumar S, Padmanabhan P, Gulyas B, Wan ACA, Rajendran VM (2018) Lineage-specific exosomes could override extracellular matrix mediated human mesenchymal stem cell differentiation. Biomaterials 182: 312-322. DOI: 10.1016/j.biomaterials.2018.08.027.

Ng CP, Sharif ARM, Heath DE, Chow JW, Zhang CBY, Chan-Park MB, Hammond PT, Chan JKY, Griffith LG (2014) Enhanced ex vivo expansion of adult mesenchymal stem cells by fetal mesenchymal stem cell ECM. Biomaterials 35: 4046-4057. DOI: 10.1016/j.biomaterials.2014.01.081.

Nieto-Nicolau N, de la Torre RM, Fariñas O, Savio A, Vilarrodona A, Casaroli-Marano RP (2020) Extrinsic modulation of integrin α6 and progenitor cell behavior in mesenchymal stem cells. Stem Cell Research 47: 101899 DOI: 10.1016/j.scr.2020.101899.

Pei M, He F (2012) Extracellular matrix deposited by synovium-derived stem cells delays replicative senescent chondrocyte dedifferentiation and enhances redifferentiation. Journal of Cellular Physiology 227: 2163-2174. DOI: 10.1002/jcp.22950.

Pei M, He F, Kish VL (2011) Expansion on extracellular matrix deposited by human bone marrow stromal cells facilitates stem cell proliferation and tissue-specific lineage potential. Tissue Engineering. Part a 17: 3067-3076. DOI: 10.1089/ten.TEA.2011.0158.

Pittenger MF, Mackay AM, Beck SC, Jaiswal RK, Douglas R, Mosca JD, Moorman MA, Simonetti DW, Craig S, Marshak DR (1999) Multilineage potential of adult human mesenchymal stem cells. Science (New York, N.Y.) 284: 143-147. DOI: 10.1126/science.284.5411.143.

Prewitz MC, Seib FP, von Bonin M, Friedrichs J, Stißel A, Niehage C, Müller K, Anastassiadis K, Waskow C, Hoflack B, Bornhäuser M, Werner C (2013) Tightly anchored tissue-mimetic matrices as instructive stem cell microenvironments. Nature Methods 10: 788-794. DOI: 10.1038/nmeth.2523.

Pricola KL, Kuhn NZ, Haleem-Smith H, Song Y, Tuan RS (2009) Interleukin-6 maintains bone marrow-derived mesenchymal stem cell stemness by an ERK1/2-dependent mechanism. Journal of Cellular Biochemistry 108: 577-588. DOI: 10.1002/jcb.22289.

Ragelle H, Naba A, Larson BL, Zhou F, Prijić M, Whittaker CA, Del Rosario A, Langer R, Hynes RO, Anderson DG (2017) Comprehensive proteomic characterization of stem cell-derived extracellular matrices. Biomaterials 128: 147-159. DOI: 10.1016/j.biomaterials.2017.03.008.

Rauch A, Haakonsson AK, Madsen JGS, Larsen M, Forss I, Madsen MR, Van Hauwaert EL, Wiwie C, Jespersen NZ, Tencerova M, Nielsen R, Larsen BD, Röttger R, Baumbach J, Scheele C, Kassem M, Mandrup S (2019) Osteogenesis depends on commissioning of a network of stem cell transcription factors that act as repressors of adipogenesis. Nature Genetics 51: 716-727. DOI: 10.1038/s41588-019-0359-1.

Rozario T, DeSimone DW (2010) The extracellular matrix in development and morphogenesis: a dynamic view. Developmental Biology 341: 126-140. DOI: 10.1016/j.ydbio.2009.10.026.

Sacchetti B, Funari A, Michienzi S, Di Cesare S, Piersanti S, Saggio I, Tagliafico E, Ferrari S, Robey PG, Riminucci M, Bianco P (2007) Self-renewing osteoprogenitors in bone marrow sinusoids can organize a

hematopoietic microenvironment. Cell 131: 324-336. DOI: 10.1016/j.cell.2007.08.025.

Salasznyk RM, Williams WA, Boskey A, Batorsky A, Plopper GE (2004) Adhesion to Vitronectin and Collagen I Promotes Osteogenic Differentiation of Human Mesenchymal Stem Cells. Journal of Biomedicine & Biotechnology 2004: 24-34. DOI: 10.1155/S1110724304306017.

Sheyn D, Ben-David S, Shapiro G, De Mel S, Bez M, Ornelas L, Sahabian A, Sareen D, Da X, Pelled G, Tawackoli W, Liu Z, Gazit D, Gazit Z (2016) Human Induced Pluripotent Stem Cells Differentiate Into Functional Mesenchymal Stem Cells and Repair Bone Defects. Stem Cells Translational Medicine 5: 1447-1460. DOI: 10.5966/sctm.2015-0311.

Stolzing A, Jones E, McGonagle D, Scutt A (2008) Age-related changes in human bone marrow-derived mesenchymal stem cells: consequences for cell therapies. Mechanisms of Ageing and Development 129: 163-173. DOI: 10.1016/j.mad.2007.12.002.

Sun Y, Li W, Lu Z, Chen R, Ling J, Ran Q, Jilka RL, Chen XD (2011) Rescuing replication and osteogenesis of aged mesenchymal stem cells by exposure to a young extracellular matrix. FASEB Journal: Official Publication of the Federation of American Societies for Experimental Biology 25: 1474-1485. DOI: 10.1096/fj.10-161497.

Suo J, Zou S, Wang J, Han Y, Zhang L, Lv C, Jiang B, Ren Q, Chen L, Yang L, Ji P, Zheng X, Hu P, Zou W (2022) The RNA-binding protein Musashi2 governs osteoblast-adipocyte lineage commitment by suppressing PPARγ signaling. Bone Research 10: 31 DOI: 10.1038/s41413-022-00202-3.

Tang C, Jin C, Du X, Yan C, Min BH, Xu Y, Wang L (2014) An autologous bone marrow mesenchymal stem cell-derived extracellular matrix scaffold applied with bone marrow stimulation for cartilage repair. Tissue Engineering. Part a 20: 2455-2462. DOI: 10.1089/ten.TEA.2013.0464.

Tang C, Xu Y, Jin C, Min BH, Li Z, Pei X, Wang L (2013) Feasibility of autologous bone marrow mesenchymal stem cell-derived extracellular matrix scaffold for cartilage tissue engineering. Artificial Organs 37: E179-E190. DOI: 10.1111/aor.12130.

Tsuchida AI, Beekhuizen M, Rutgers M, van Osch GJVM, Bekkers JEJ, Bot AGJ, Geurts B, Dhert WJA, Saris DBF, Creemers LB (2012) Interleukin-6 is elevated in synovial fluid of patients with focal cartilage defects and stimulates cartilage matrix production in an in vitro regeneration model. Arthritis Research & Therapy 14: R262 DOI: 10.1186/ar4107.

Unsicker K, Spittau B, Krieglstein K (2013) The multiple facets of the TGF-β family cytokine growth/differentiation factor-15/macrophage inhibitory cytokine-1. Cytokine & Growth Factor Reviews 24: 373-384. DOI: 10.1016/j.cytogfr.2013.05.003.

Vidal MA, Kilroy GE, Johnson JR, Lopez MJ, Moore RM, Gimble JM (2006) Cell growth characteristics and differentiation frequency of adherent equine bone marrow-derived mesenchymal stromal cells: adipogenic and osteogenic capacity. Veterinary Surgery: VS 35: 601-610. DOI: 10.1111/j.1532-950X.2006.00197.x.

Vidal MA, Kilroy GE, Lopez MJ, Johnson JR, Moore RM, Gimble JM (2007) Characterization of equine adipose tissue-derived stromal cells: adipogenic and osteogenic capacity and comparison with bone marrow-derived mesenchymal stromal cells. Veterinary Surgery: VS 36: 613-622. DOI: 10.1111/j.1532-950X.2007.00313.x.

Wagner W, Bork S, Horn P, Krunic D, Walenda T, Diehlmann A, Benes V, Blake J, Huber FX, Eckstein V, Boukamp P, Ho AD (2009) Aging and replicative senescence have related effects on human stem and progenitor cells. PloS One 4: e5846 DOI: 10.1371/journal.pone.0005846.

Yang Y, Lin H, Shen H, Wang B, Lei G, Tuan RS (2018) Mesenchymal stem cell-derived extracellular matrix enhances chondrogenic phenotype of and cartilage formation by encapsulated chondrocytes in vitro and in vivo. Acta Biomaterialia 69: 71-82. DOI: 10.1016/j.actbio.2017.12.043.

Yang Y, Liu Y, Lin Z, Shen H, Lucas C, Kuang B, Tuan RS, Lin H (2019) Condensation-Driven Chondrogenesis of Human Mesenchymal Stem Cells within Their Own Extracellular Matrix: Formation of Cartilage with Low Hypertrophy and Physiologically Relevant Mechanical Properties. Advanced Biosystems 3: e1900229 DOI: 10.1002/adbi.201900229.

Yong I, Oh SW, Kim P (2020) Re-engineered cell-derived extracellular matrix as a new approach to clarify the role of native ECM. Methods in Cell Biology 156: 205-231. DOI: 10.1016/bs.mcb.2019.12.007.

Yuan M, Yeung CW, Li YY, Diao H, Cheung KMC, Chan D, Cheah K, Chan PB (2013) Effects of nucleus pulposus cell-derived acellular matrix on the differentiation of mesenchymal stem cells. Biomaterials 34: 3948-3961. DOI: 10.1016/j.biomaterials.2013.02.004.

Zhang W, Zhu Y, Li J, Guo Q, Peng J, Liu S, Yang J, Wang Y (2016) Cell-Derived Extracellular Matrix: Basic Characteristics and Current Applications in Orthopedic Tissue Engineering. Tissue Engineering. Part B, Reviews 22: 193-207. DOI: 10.1089/ten.TEB.2015.0290.

Zupan J, Strazar K, Kocijan R, Nau T, Grillari J, Marolt Presen D (2021) Age-related alterations and senescence of mesenchymal stromal cells: Implications for regenerative treatments of bones and joints. Mechanisms of Ageing and Development 198: 111539 DOI: 10.1016/j.mad.2021.111539.

Editor's note: The Scientific Editor responsible for this paper was Fergal O' Brien.